Nonlinear Experimental Estimation and Verification of a MIMO System through EKF

A. Kulkarni, S. Purwar
Motilal Nehru National Institute of Technology,
Allahabad , India, arkulkarni17@gmail.com, shubhi@mnnit.ac.in

Abstract: *Twin Rotor Multi Input Multi Output System (TRMS) is a highly nonlinear laboratory experimental model of helicopter. Real time experimental results are presented to prove the Extended Kalman Filter (EKF) observer performance in terms of estimation error convergence along with the Lyapunov stability analysis. The RMS error of the proposed EKF observer is compared with the previously published local state observer and neural observer estimation results* [2]. *Further an algorithm previously published in* [19] *is applied in real time TRMS and its RMS error are compared with earlier results. It is found that the proposed observer estimation errors for pitch angle and yaw angle are less than the earlier results. The efficient results are outcome of Matlab Simulink with Real time Windows target hardware–software interface. Robustness of the estimator is verified with the externally generated manual disturbance and against an unknown indirect surge in mains supply of the TRMS hardware. It was observed that the estimation errors are within 2 sigma limits. Further it is observed that wherever the slope of the pitch and yaw angle is fast, the estimation error section is denser and the time taken for estimation is less and vice versa.*

Key words: *Nonlinear system, Observer, pitch angle, yaw angle, jacobian.*

1. Introduction.

Measurement of pitch angle, yaw angle and their respective rates are important aspects of helicopter safety. Exceeding safe pitch angle, bank angle, and permissible smooth flight transactions than the operating standards may result into an accident. The Twin Rotor Multi Input Multi Output system (TRMS) is one of the helicopter models [1] which provide an experimental facility to researchers. To have sufficient description of the nonlinear model of TRMS; however, one requires state parameters such as pitch and yaw angles and their velocities, momentum of main and tail rotor etc. Such sensors either are difficult to manufacture, or even if available, are costly and may occupy additional space in the hardware. This inspires us to go for design of observers. An effort in this direction is done in [2]. In [2] unknown nonlinearities of the TRMS system were estimated using Chebyshev neural network (CNN); whereas in local state observer the system model was assumed to be completely known. Thus a comparison based on RMS errors of pitch and yaw angle estimation was of concern there.

The versatility of Kalman filters and its variations in *real time* is described briefly in the forthcoming lines. In [3], based on the known uncertainties in terms of passive sonar bearing measurements, and position of SSBN track, along with SSN's velocities; EKF is used to provide submarine track rebuilding. It was mentioned that prediction error disparity could be minimized by knowledge of *correlated noise and bias* in the sonar uncertainty model. Aerospace systems are imputed as nonlinear models accompanied with noisy and biased transducers measurements. EKF is accepted as one of the most popular nonlinear filtering technique in the aerospace industry [4]. In [5], the EKF is applied as estimator to get comprehensive signaling about lack of proportion of the absolute vanadium concentration in vanadium redox flow batteries (VRFB). Estimation of induction motor flux and velocity under the variations of stator and rotor resistances inclusive of load torque and velocity changes is done in a novel way [6]. By sequentially deploying two EKFs at each time step (braided technique) authors overcomes the problem of decreased-estimation-accuracy. Kalman Filter is implemented in real time estimation of velocity of a mechanical motion system and results obtained are compared with those of moving horizon polynomial fitting method [7]. In another gigantic area of power systems, voltage magnitude and phase angle (*static states*) after estimation are fed to a primary Kalman filter. These results are then passed to second stage EKF which estimates generator rotor angles and speeds (*dynamic states*) [8].Comparison of EKF with Invariant EKF is presented in [9]. In [10], EKF is integrated to achieve map matching by comparing scans experimentally in Simultaneous Localization and Mapping (SLAM) framework. In [11], aptness of *cascaded* EKF is proved for tractor yaw control against hitch load variations based on finding a method when considerable instigate yaw dynamics

is present. The detailed explanation about most important properties of filter such as convergence, degree of stability associated with errors at starting condition can be found in [12]. In [19], a little modification in the EKF is done to treat nonlinearities in induction machines effectively through flux and angular velocity estimation. That work was supported by practical usefulness of observer. A scalar constant was used to modify the Riccati differential equation. This scalar constant takes the form of a real square diagonal matrix for multi-input-multi-output (MIMO) systems. The algorithm in [19] is redesigned for TRMS helicopter model and applied in real time TRMS experimental system. The RMS values of pitch and yaw angles are compared with two other algorithms in earlier published literature [2]. However, such complex interacting nonlinear systems should be tested with response to noise added to either sensors, or to process or both. Kalman filters have the advantage of rejecting the noise at the same time they provide estimation as well. In the literature, no work has been reported on application of EKF for estimation of pitch and yaw angles of TRMS.

Organization of the paper is as follows. In Section 2, description of the TRMS is given in terms of set of differential equations. Section 3 shows the test for local observability. Problem statement and EKF observer is explained in Section 4, whereas Lyapunov stability analysis is given in Section 5. In Section 6 experimental results of the proposed EKF observer-estimator and experimental results based on algorithm-"EKF based nonlinear observer with a prescribed degree of stability" in [19] (please see Section 6.1 and 6.2). Further robustness test against unknown surge and externally manually created disturbance is given in the same section. Section 7 has discussions in terms of degree of stability and tuning. Last Section 8 concludes the work.

2. About System

We consider the system in the form [13]

$$\begin{aligned} \dot{x} &= f(x(\mathrm{t}),u,t)+w(\mathrm{t}) \\ z(\mathrm{t}) &= h(x(\mathrm{t}),t)+v(\mathrm{t}) \end{aligned} \qquad (1)$$

where

$$x=\begin{bmatrix}\psi & \dot{\psi} & \varphi & \dot{\varphi} & \tau_1 & \tau_2\end{bmatrix}^T,$$
$$u=\begin{bmatrix}u_1 & u_2\end{bmatrix}^T, z=\begin{bmatrix}\psi & \varphi\end{bmatrix}^T$$

are state, input and measurement vectors respectively; f and h are continuous functions of time and $v\in\mathbb{R}^p, w\in\mathbb{R}^q$ are vectors of independent uncorrelated continuous random variables with mean zero and covariance R and Q respectively. Further we refer system from [2].

$$\begin{aligned}
\dot{x}_1 &= x_2 + w_1(t) \\
\dot{x}_2 &= \left(\frac{a_1}{I_1}x_5^{\,2}\right)+\left(\frac{b_1}{I_1}x_5\right)-\left(\frac{M_g}{I_1}sin(x_1)\right)-\left(\frac{B_{1\psi}}{I_1}x_2\right) \\
&+\left(\frac{0.0326}{2I_1}\right)sin\left((2x_1)x_4^{\,2}\right)-\left(\frac{k_{gy}a_1}{I_1}\right)\left(cos(x_1)x_4x_5^{\,2}\right) \\
&+\left(\frac{k_{gy}b_1}{I_1}\right)cos(x_1)x_4x_5\dot{x}_2+w_2(t) \\
\dot{x}_3 &= x_4 + w_3(t) \\
\dot{x}_4 &= \left(\frac{a_2}{I_2}\right)x_6^{\,2}+\left(\frac{b_2}{I_2}\right)x_6-\left(\frac{B_{1\phi}}{I_2}\right)x_4-\left(\frac{1.75k_ca_1}{I_2}\right)x_5^{\,2} \\
&-\left(\frac{1.75k_cb_1}{I_2}\right)x_5+\left(\frac{0.375k_ca_1}{I_2}\right)\exp(-0.5t)\,x_5^{\,2} \\
&+\left(\frac{0.375b_1k_c}{I_2}\right)x_5\exp(-0.5t)+w_4(t) \\
\dot{x}_5 &= -0.833x_5+\left(\frac{\mathrm{k}_1}{\mathrm{t}_{11}}\right)\mathrm{u}_{\mathrm{a}0}+w_5(t) \\
\dot{x}_6 &= -x_6+\left(\frac{\mathrm{k}_2}{\mathrm{t}_{21}}\right)\mathrm{u}_{\mathrm{b}0}+w_6(t)
\end{aligned} \qquad (2)$$

where the constants are as given below [1]

$$a_1=0.0135; a_2=0.02; b_1=0.0924; b_2=0.09; B_{1\psi}=0.006;$$
$$B_{1\phi}=0.1; I_1=0.068; I_2=0.02; k_c=-0.2; k_{gy}=0.05;$$
$$k_1=1.1; k_2=0.8; M_g=0.32.$$

3. Observability Test

Before we design observer, the system observability must be proven. It was revealed in [14] that *local observability* is inference of quiddity of full rank (i.e. $\dim dO(x_0)=n$, where n is the dimension of the output). The observability vector $O(x)$ for above system becomes

$$O(x)=\begin{bmatrix}y & \dot{y} & \ddot{y} & \dddot{y}\end{bmatrix}^T \qquad (3)$$

where the output vector is $y=\begin{bmatrix}x_1 & x_3\end{bmatrix}^T$

The Jacobian matrix is

$$dO(x)=\begin{bmatrix}
1 & 0 & 0 & 0 & 0 & 0 \\
0 & 0 & 1 & 0 & 0 & 0 \\
0 & 1 & 0 & 0 & 0 & 0 \\
0 & 0 & 0 & 1 & 0 & 0 \\
R_{51} & R_{52} & R_{53} & R_{54} & R_{55} & R_{56} \\
R_{61} & R_{62} & R_{63} & R_{64} & R_{65} & R_{66}
\end{bmatrix}^T \qquad (4)$$

where $R_{5k}=\dfrac{\partial\dot{x}_2}{\partial x_i}$; $R_{6k}=\dfrac{\partial\dot{x}_4}{\partial x_i}$ $\quad i=1,\ldots 6$.

When system possesses equilibrium zero, the rank becomes five, i.e. at rest; however, for other than zero equilibrium, the rank is six. Hence we can say that the system is locally observable and the road to observer design is clear.

4. Problem Statement and EKF observer

Continuous time EKF Estimator dynamics [14] is as given below by the stochastic model:

$$\begin{aligned}
&\dot{\hat{x}}(\mathrm{t}) = f(\hat{\mathrm{x}}(\mathrm{t}), u, \mathrm{t}) + \mathrm{K}(t)[z(\mathrm{t}) - \hat{z}(\mathrm{t})] \\
&\hat{z}(\mathrm{t}) = h(\hat{x}(\mathrm{t}), \mathrm{t}) \\
&K(\mathrm{t}) = P(\mathrm{t})H^T(\hat{x}(\mathrm{t}), t)R^{-1}(\mathrm{t}) \\
&\dot{P}(\mathrm{t}) = F(\hat{x}(\mathrm{t}), t)P(\mathrm{t}) + P(\mathrm{t})F^T(\hat{x}(\mathrm{t}), \mathrm{t}) + Q(\mathrm{t}) \\
&-P(\mathrm{t})H^T(\hat{x}(\mathrm{t}), \mathrm{t})R^{-1}(\mathrm{t})H^T(\hat{x}(\mathrm{t}), \mathrm{t})P(\mathrm{t}) \qquad (5)
\end{aligned}$$

Where $\hat{x}$ represents the estimated states, $F = \frac{\partial}{\partial x}(f)$ and $H = \frac{\partial}{\partial x}(h)$ evaluated with current estimated states, $K(t)$ is Kalman gain of continuous time EKF, $P(t)$ error covariance matrix. It should be noted that this matrix is to be obtained by solving the Riccati matrix differential equation in real time. Continuous time EKF assumes coupling of the prediction-correction mechanism for discrete EKF. Further it is to be noted that there is nonlinear function in plant but the relationship in output is linear.

The local state observer in [2] is computationally less complex than the online Kalman gain computation and solving differential Riccati equation online, however such computational complexity is justified because of the fast convergence of the estimation error to a bounded finite set of values. Following assumptions are used to design an EKF for TRMS.

4.1 Assumptions

1) Approximation of f are acceptable near equilibrium points so that the Jacobian exists.

2) Uncertainties (standard deviations associated with each state variable) are known which are further expressed in terms of $\left(\sigma_{\varphi}, \sigma_{\dot{\varphi}}, \sigma_{\phi}, \sigma_{\dot{\phi}}, \sigma_{\tau_1}, \sigma_{\tau_2}\right)$.

3) Measurement and Process Noise Covariance matrices are known.

With consideration of system dynamics in equation (2) and assumptions mentioned above, one then seek to find estimates of pitch and yaw angles so that the RMS estimation error is minimized or in other words one seeks to find Kalman gain that causes the error covariance be bounded [15]. The objective is also to implement in the real time environment for verification of the experimental results. Major reasons for use of EKF in real time implementation [16] are scanty computational load [17] and its simplicity. One may refer [18] to get the interesting profundity of EKF dynamics.

The process noise matrix Q and sensor noise matix R have their diagonal elements as given below: $\{0.0099 \quad 0.0022 \quad 0.0894 \quad 0.0017 \quad 1.2678 \quad 1.2700\}$ and $\{0.0007 \quad 0 \; 0.00193\}$ respectively. The initial value of error covariance matrix is assumed as diagonal matrix whose diagonal elements are taken as

$\gamma\{1.0500 \quad 0.0500 \quad 1.0000 \quad 1.0000 \quad 1.0000 \quad 1.0000\}$

where $\gamma > 0$ is a constant.

5. Stability Analysis

Now following [19] for stability analysis; except one change is that, freedom parameter is not taken into consideration.

Let the estimation error be defined as below:

$$\xi = x - \hat{x} \qquad (6)$$

Differentiating equation (6) one gets:

$$\dot{\xi} = \left[F - KH\right]\xi + \phi(x, \hat{x}) - K\,\rho(x, \hat{x}) \qquad (7)$$

where $\phi(x, \hat{x}), \rho(x, \hat{x})$ are terms of second and higher order in power series expansion of $f(\bullet), h(\bullet)$ respectively. Let us proceed with few important definitions and some assumptions before stating main theorem.

5.1 Definition 1

The equilibrium $\xi = 0$ of equation (7) is exponentially stable if $\eta, \theta > 0$ such that

$$\|\xi\| \le \eta\|\xi(0)\|\exp(-\theta t) \qquad (8)$$

holds for every $t > 0$ and for every solution of $\xi(\bullet)$

5.2 Definition 2

The observer given by (5) is exponential observer if the estimation error differential equation (7) has an exponential stability of equation (8).

5.2.1 Assumption 1

The following nonlinearities are bounded

$$\begin{aligned}
&\|\phi\| \le G_{\phi}\|x - \hat{x}\|^2 \\
&\|\rho\| \le G_{\rho}\|x - \hat{x}\|^2 \qquad (9)
\end{aligned}$$

such that $G_{\phi}, G_{\rho} > 0$ for $x, \hat{x} \in R^n$.

Also the inequality is regenerated from [19] here without proof

$$\xi\Upsilon\phi(x, \hat{x}) - \xi^T\Upsilon\rho(x, \hat{x}) \le \kappa\|\xi\|^3 \qquad (10)$$

where $\Upsilon = P^{-1}$ and $\kappa > 0$ is a constant, above proof can be verified along with following relation where p_l defined later.

$$\kappa = \frac{G_{\varphi}}{p_l} + \frac{\bar{b}G_{\rho}}{\varpi} \qquad (11)$$

where $\varpi > 0$ is a constant.

5.2.2 Assumption 2 [24]
For efficient estimation F is bounded with following condition.

$$\|F\| \le \bar{b} \tag{12}$$

where $\bar{b} > 0$.

5.2.3 Assumption 3

The Riccati differential equation mentioned in (5) has bounds on error covariance matrix:

$$p_l I \le P \le p_h I \tag{13}$$

where $p_l, p_h > 0$

Theorem
With $\alpha > 0$, Q, R as positive definite matrices, the proposed observer in equation (5) is an exponential observer.

5.2.4 Proof
With reference to estimation error equation (6), the exponential stability without free parameter can be proven.
Let a Lyapunov function be selected as

$$V(\xi) = \xi^T \Upsilon \xi \tag{15}$$

with $\Upsilon = P^{-1}$
The time derivative of above Lyapunov function is

$$\dot{V} = \dot{\xi}\Upsilon\xi + \xi^T \dot{\Upsilon}\xi + \xi^T \Upsilon \dot{\xi} \tag{16}$$

$$\dot{\Upsilon} = -\Upsilon \dot{P} \Upsilon. \tag{17}$$

Substitute equation (7) in (16) with application of equation (10), one get:

$$\dot{V} \le -\xi^T \left[\Upsilon Q \Upsilon + H^T R^{-1} H \right] \xi \tag{18}$$

Let

$$Q = q_a I \tag{19}$$

Additionally note that $\Upsilon = P^{-1} \Rightarrow \Upsilon^2 = \frac{1}{p_h^{\,2}}$, following is obtained:

$$\therefore \dot{V} \le -\xi^T \left[\frac{q_a}{p_h^2} + H^T R^{-1} H \right] \xi \tag{20}$$

for $\|\xi\| \le \varepsilon_d$ with $\varepsilon_d = \min\left(\varepsilon, \frac{q_a}{\mu\, p_h^2} \right)$ where $\varepsilon, \mu > 0$ are constants.
This proves the local negative definiteness.
As

$$\dot{V} \le -\frac{q_a}{p_h^2} V \tag{21}$$

where

$$V = \frac{1}{p_l} \|\xi\|^2 \tag{22}$$

$$\therefore V\left(\xi(t), t\right) = V\left(\xi(0), 0\right) \exp\left(\frac{-q_a}{p_h^2} \right) \tag{23}$$

$$\therefore \|\xi\| \le \kappa \|\xi(0)\| \exp\left(\frac{-q_a}{p_h^2} \right) \qquad \kappa > 0 \tag{24}$$

Let

$$\Xi = \kappa \|\xi(0)\| \exp\left(\frac{-q_a}{p_h^2} \right) \tag{25}$$

With reference to [13]; the above term bonds initial error convergence and degree of stability. With this in the forthcoming sessions experimental results are presented.

6. Real Time Experimental Results

6.1 Results with standard Pdot

We call the algorithm mentioned in equation (5) as standard Pdot for simplicity. The experimental verification is done with Feedback Instruments 33-949 Matlab Simulink Models and Windows Real Time target software in External mode for a run time of 30 s. The PC used is Intel (R) core (TM) 2 CPU 6320 @1.86 GHz, 2.48 GB of RAM. There are two integrators used in the experiment. One is for matrix Riccati differential equation and other is for estimation differential equation as shown above. The initial condition for matrix Riccati differential equation is as shown above with initial condition source as 'internal' and its upper and lower saturation limits are given as ± 10. For the integrator used for state estimation differential equation the upper saturation limit is set as ± 0.5. The initial condition source has to be given internally in the external mode for real time interfacing. Advantech PCI 1711 I/O board is used with sample time of 0.001s. Both the channels of encoders (for pitch and yaw angles) have offset set as zero. Various control signals are used in simulation mode for testing purpose. They are treated as simple sinusoid, multi-sinusoid and exponential signals. For simple sinusoid the control signal is $u = \left[0.2\sin(0.4t) \quad 0.2\sin(0.4t) \right]^T$ and for exponential control $u = \left[0.1\left(1 - \exp(-0.8t)\right) \quad 0.1\left(1 - \exp(-0.8t)\right) \right]^T$ and for multi-sinusoid

$$u = \begin{bmatrix} 0.2\sin(0.4t) + 0.4\sin(0.6t) + 0.05\sin(0.8t) \\ 0.2\sin(0.4t) + 0.4\sin(0.6t) + 0.05\sin(0.8t) \end{bmatrix}.$$

It should be noted that the exponential control signals produces considerably large variations in yaw angle and hence should *not* be used in real time experimentation. For real time experimental estimation multi-sinusoid signals are used. The control signals are applied in open loop system. The pitch and yaw angle estimations are plotted within ± 2 sigma limits of normalized errors. The initial condition for the plant and estimator is taken as

$$x = \begin{bmatrix} 0 & 0 & 0 & 0 & 0 & 0 \end{bmatrix}^T$$

shown

$$\hat{x} = \begin{bmatrix} 0.05 & 0 & -0.05 & 0 & 0 & 0 \end{bmatrix}^T$$

Figure 1 and 2 shows the estimated and true states in open loop response for multi-sinusoidal control signals given to main rotor (pitch motor) and tail rotor (yaw angle). It can be observed from the figure 1 that the estimation error $(\hat{x} - x)$ amplitude remains bounded around zero to a small finite set of values. Denser sections of error (see figure 3 and figure 4) are associated with small prediction time that causes increase in average error magnitude, whereas wider sections of the error can be observed near time when pitch angle changes its transition and thus causing reduction in average error.

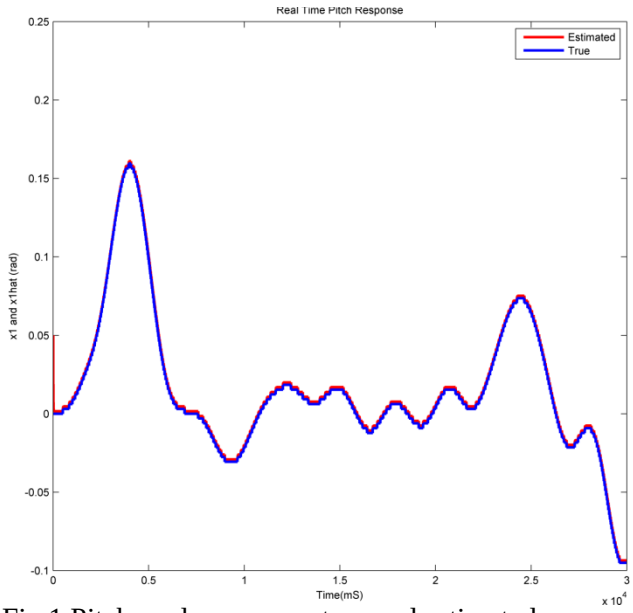

Fig.1 Pitch angle response-true and estimated

This can be well observed in figure 12 and 13 in the microscopic view. The yaw response seems to be smoother than the pitch response (see figure 2). The range of the yaw angle is larger than that of the pitch angle. This automatically puts a necessity on the yaw encoder to have greater resolution than that of pitch encoder. Also the interaction between yaw angle and pitch rotor exits which is reason for the non-minimum phase-type behavior of the TRMS.

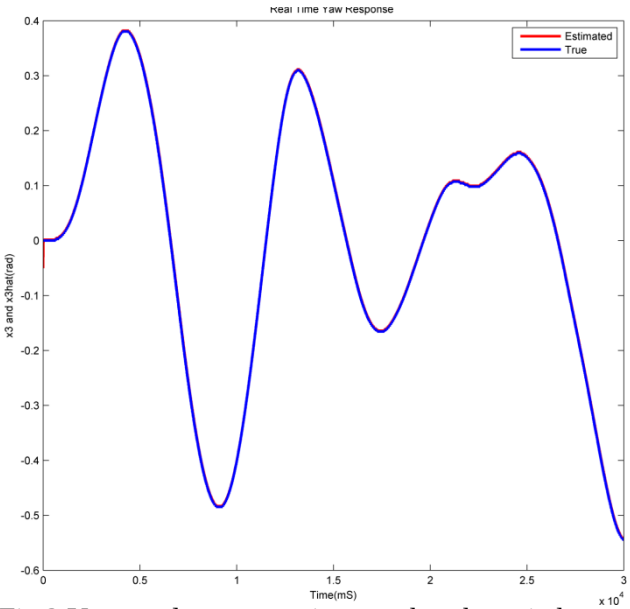

Fig.2 Yaw angle response is smoother than pitch

Various measurement noise values are selected by experimental testing and the response is shown in figure 5 and 6. It should be noted that the limits of the integrator causes saturation in the yaw response to clip at 0.5 rad (see figure 6).Such limitations are necessary if any corrective action is to be taken based on estimation (for example controling action on any of the states) in future work. Measurement noise1 values are $\begin{bmatrix} 0.000235 & 0.000800 \end{bmatrix}$.Other measurement noise values tested were $\begin{bmatrix} 0.010000 & 0.060000 \end{bmatrix}$.

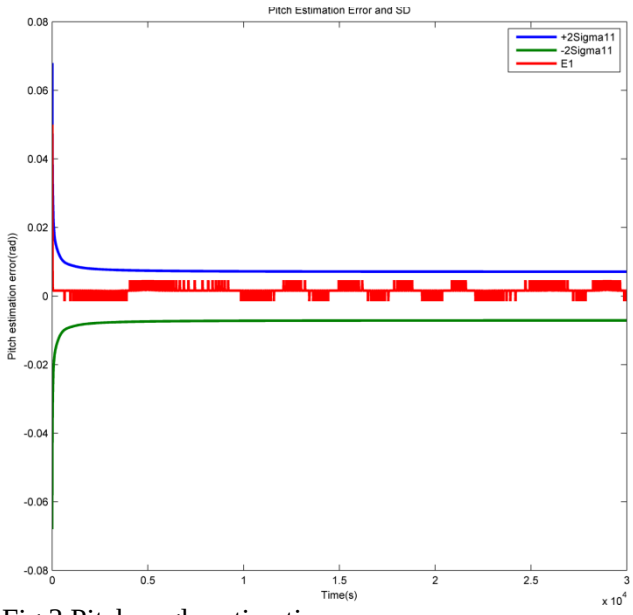

Fig.3 Pitch angle estimation error

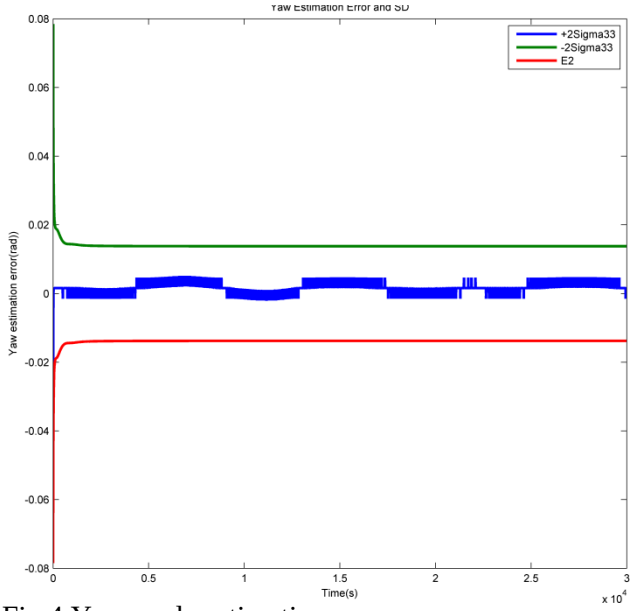

Fig.4 Yaw angle estimation error

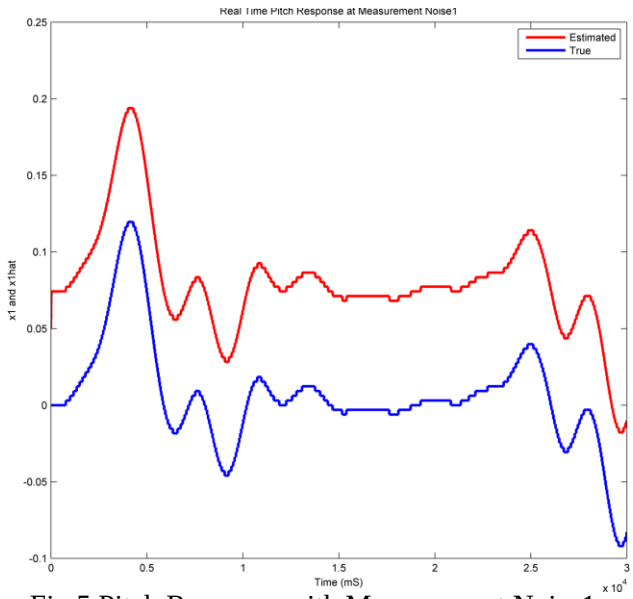

Fig.5 Pitch Response with Measurement Noise1

As these values increases, the estimated values moves on the upside and cause saturation, and should be avoided. Similarly it is observed that if the process noise matrix Q is taken as 100 times the value assumed at the end of Section 3, then the estimation error in pitch angle increases considerably (i.e. about ± 0.1 rad), whereas the yaw angle error is about ± 0.05 rad. Now the experimental results of modified Pdot are presented.

6.2 Experimental results of modified Pdot

In [19] an alogrithm named "an EKF based nonlinear observer with a prescribed degree of stability" is discussed. The reason behind calling this as modified Pdot is clarified in the Riccati differential equation in [19] which is given below:

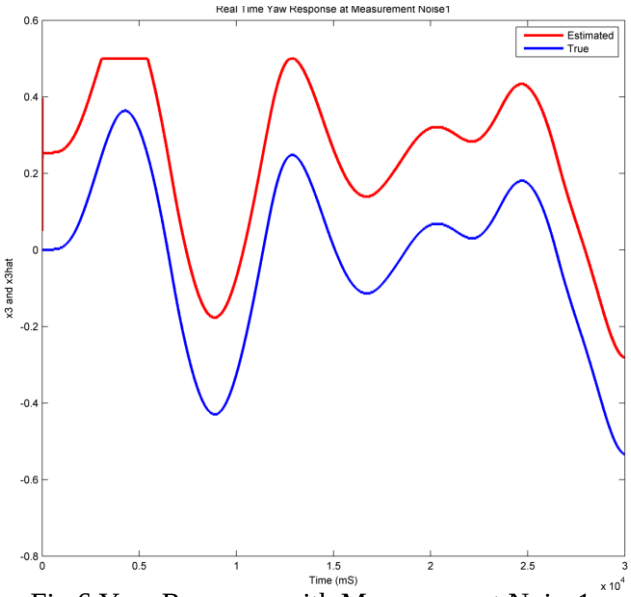

Fig.6 Yaw Response with Measurement Noise1 because of integrator saturation limit exceeded

$$\dot{P}(\mathrm{t}) = (F(\hat{x}(\mathrm{t}), t) + \alpha I)P(\mathrm{t}) + P(\mathrm{t})(F^T(\hat{x}(\mathrm{t}), \mathrm{t}) + \alpha I) + Q(\mathrm{t}) - P(\mathrm{t})H^T(\hat{x}(\mathrm{t}), \mathrm{t})R^{-1}(\mathrm{t})H^T(\hat{x}(\mathrm{t}), \mathrm{t})P(\mathrm{t}), \quad \alpha > 0 \qquad (26)$$

In [19] the purpose of modification was explained on the basis of degree of stability in advance and effective treatment of nonlinearities. This is a kind of modified EKF nonlinear observer with an additive term of instability [19]. It should be noted that such algorithm can be applied on nonlinear system however there is no nonlinear relationship in output function. Here one generalizes local exponential stability of equation (8). Further the real constant α in [19] is a scalar quantity. In order to implement the modified Pdot algorithm for TRMS, this becomes a real square diagonal matrix. By experimental trials this matrix is taken as $diag\{0.01 \quad 1 \quad 0.0000300 \quad 1 \quad 1 \quad 1\}$. Now this modified algorithm which takes the name of *modified Pdot* is applied on the nonlinear TRMS. The results are given below.

From both the responses (figure 7 and figure 8) it is clear that there is a kind of phase lag between the true and estimated states. If the constant α matrix is made zero then the algorithm becomes a standard Pdot algorithm.

The robustness performance of the estimator is tested in two ways. A real unknown magnitude surge is reflected on power supply of TRMS. This surge however does not make any reflection on control signal coming from PC. The reason is assumed as the Switch Mode Power Supply of the PC did not pass the surge to control signal.

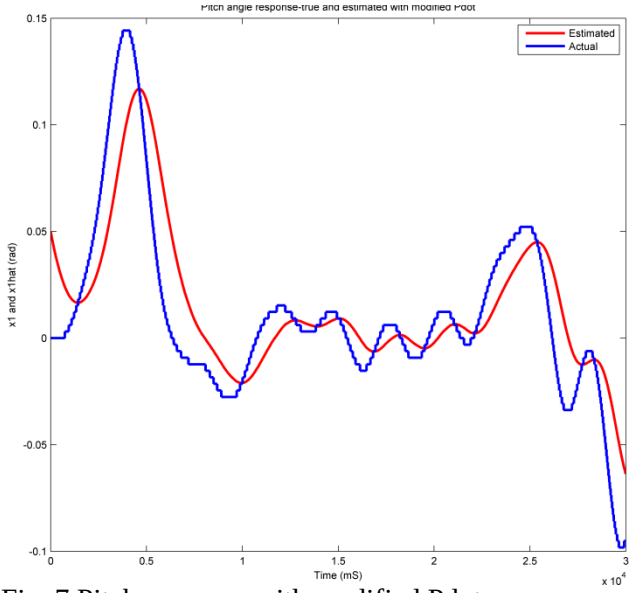

Fig. 7 Pitch response with modified Pdot

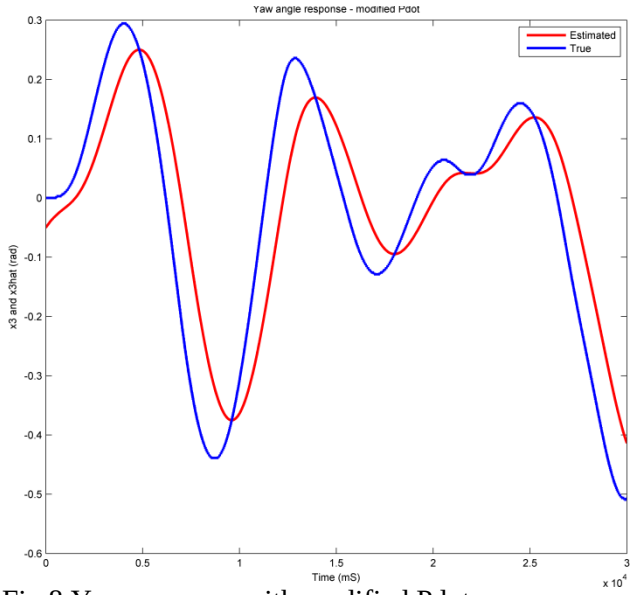

Fig.8 Yaw response with modified Pdot

As the surge is outcome of various unknown loads connected in parallel, its magnitude could not have been detected nor is such arrangement available in the experimental set up.
Still thankfully the surge is reflected in the response. The surge effect is shown in figure 9 and 10 where as figure 11 shows control signal pattern. The surge came at after 25 s and there is a sudden uplift in pitch angle**.** The yaw response in this case is seen more sensitive. The estimator response can be said satisfactory in this unknown surge case.
Secondly a manual external disturbance is exerted in vertical direction whose magnitude is about 0.2 rad. This will cause oscillations in pitch angle. However there is almost nil effect however on the yaw angle as the disturbance do not affect the horizontal direction. In both cases the estimator performance is better to test robustness. For all the cases of experiments the control signal is same as shown in figure 9.

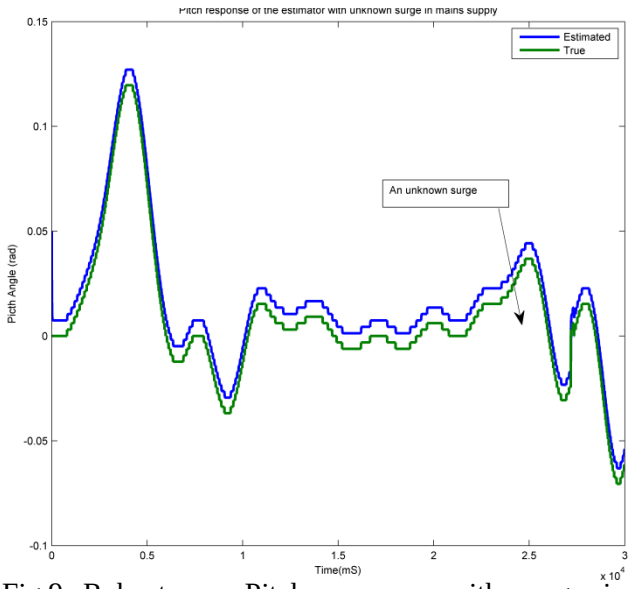

Fig.9 Robustness: Pitch response with surge in mains supply of TRMS hardware**.**

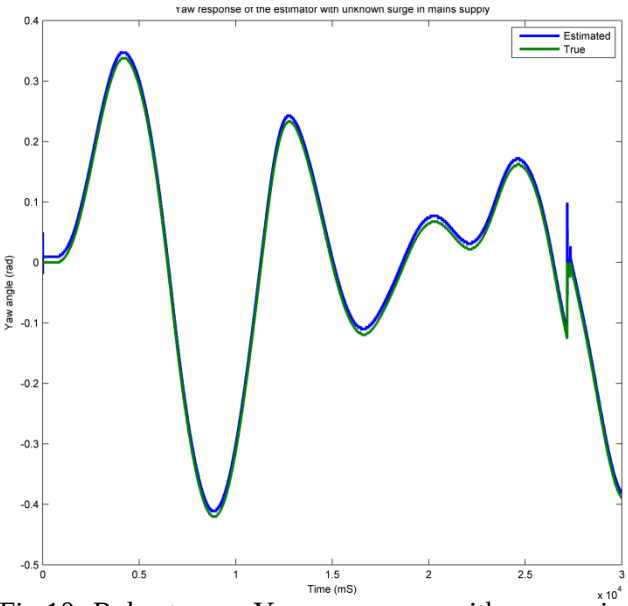

Fig.10 Robustness: Yaw response with surge in mains supply of TRMS hardware.

Figure 12 and 13 are the microscopic view of the pitch and yaw response taken when the initial position is slightly different, which shows the mechanism of prediction –correction in EKF. It can be clearly seen how the error magnitude and the time between the two predictions changes as the slope of the pitch or yaw angle changes while going through zero angle or during transition from positive or negative peak. Because of the space limitation the responses of the estimator for other initial conditions

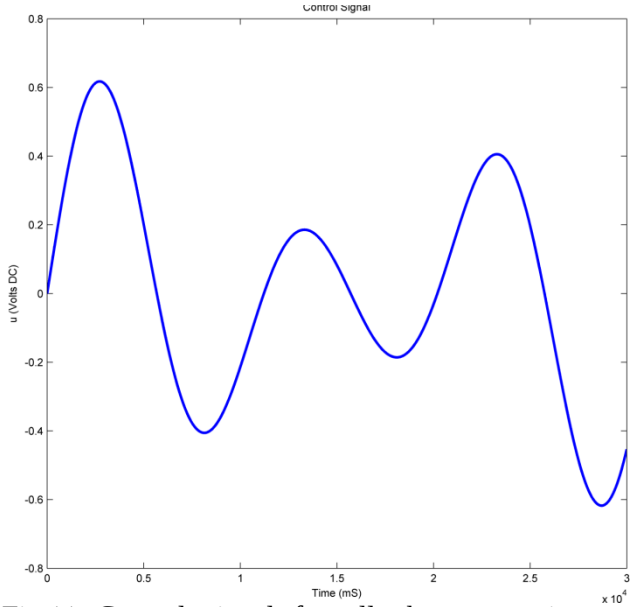

Fig.11 Control signal for all above experiments given to both motors (i.e. main and tail rotor)

as well as various set of control signals are represented here.

The effect of process noise can be verified in a different way by only making change in individual element of process noise matrix. The initial value of error covariance matrix is considerably greater than the process noise matrix. This result in a sharp transition in reduction of estimation error .This also can be observed by plotting the *trace* of error covariance matrix. Though the error plots are given here of pitch and yaw angle, it is possible to have similar plots of all the variables of the systems, however one need in that case the operating range of the respective state variables. Un-availability of the statistical characteristics of the sensors is one of the hurdles in detail analysis and design of EKF.

An external manual disturbance of magnitude 0.2 rad in vertical direction is generated and its associated response is shown in figure 14 and 15.

If such disturbance is to be generated in horizontal direction, then there will be negligible variations in yaw response.

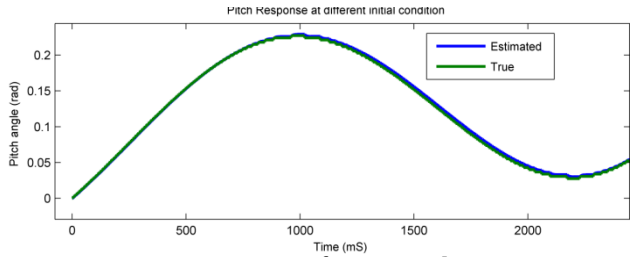

Fig.12 Microscopic view of EKF pitch estimation

For comparison, the performance of Local state observer and Neural observer RMS pitch and yaw errors published in [2] is compared with the proposed two estimators: estimation with standard Pdot and with modified Pdot and given below in Table 1 (see next page). E_{1rms} and E_{3rms} are the RMS estimation errors associated in pitch and yaw angles respectively.

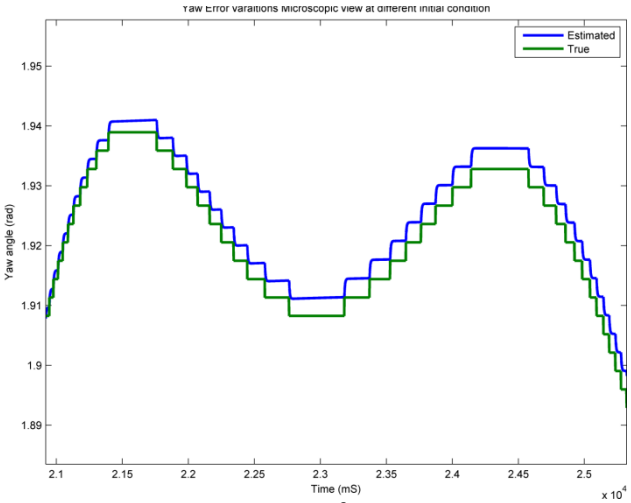

Fig.13 Microscopic view of EKF yaw estimation: the estimation error amplitude as well as time taken for estimation is minimum for larger slope and vice versa

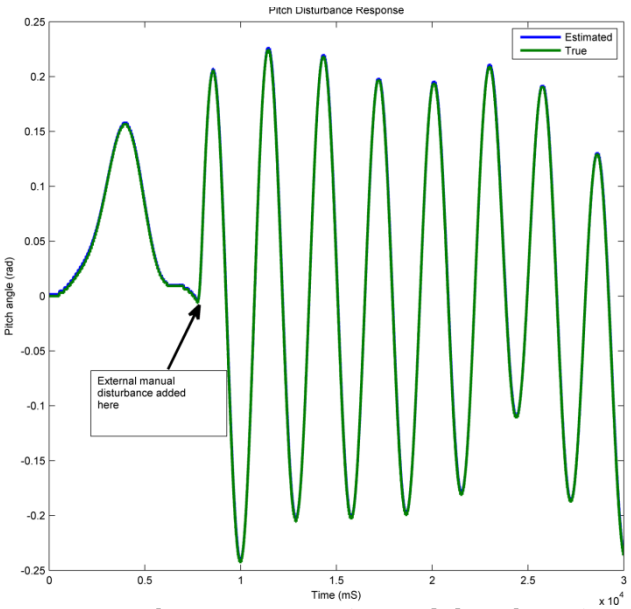

Fig.14 Disturbance response (manual disturbance) in upward direction of magnitude about 0.2 rad causing oscillations in pitch angle

Because of the space limitations the error plots are given here. Further the speed of convergence in both the algorithms can be compared. That can be treated as future scope. From this comparison it is clear that the additional computational complexity in EKF because of online Jacobian solving is compensated by reduction in estimation error.

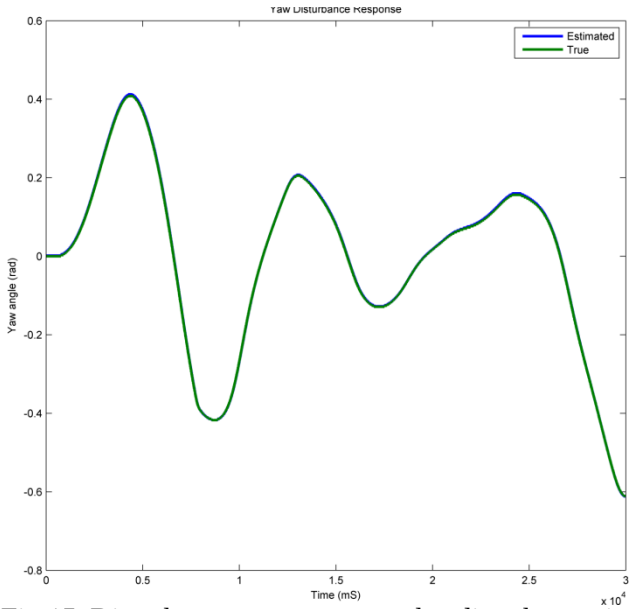

Fig.15 Disturbance response: as the disturbance is acting vertically, the yaw response is not much affected

Table 1
Comparison of RMS estimation error algorithms

Observer	E_{1rms}	E_{3rms}
Local State Observer [2]	0.0040	0.0263
Neural Observer [2]	0.0023	0.0088
Proposed EKF observer	0.0016	0.0017
With modified Pdot	0.0016	0.0018

7 Discussions

7.1 Degree of Stability

It was pointed in [20] that the dive of initial error $\zeta(0)$ is rightly affiliated to the degree of stability. The bigger the degree of stability, quicker Ξ converges to zero at the early state. From the estimation error plots (i.e. figure 3 and figure 4); it is clear that the degree of stability is large. It was also pointed in [20] that if $\bar{q}$ was zero, which indicates question mark on degree of stability confidence. Note that EKF may diverge if we test it for higher control signal amplitudes or frequencies or with different set of initial conditions, resulting in oscillatory response.

7.2 Tuning

Getting feasible covariance matrix elements need repetitive tuning based on observed filter response [21]. We also have selected the tuning parameters after several trials. Also an eency value of system noise covariance matrix for upswing in EKF applicability is one of the plenty of options [22]; specifically the case when one do not have statistical characteristics of sensors.

8 Conclusions

We present a standard EKF observer for a multi input multi output TRMS. Practical real time experimental results are shown to prove the applicability of EKF. It was observed that the estimation errors are within 2 sigma limits. Robustness of the estimator is checked against an unknown surge in mains supply of the TRMS hardware and externally manually generated disturbance of considerable magnitude. The disturbance response is satisfactory. The degree of stability of observer is demonstrated with estimation error convergence towards zero. Considerable reduction in RMSE has been obtained with the proposed EKF in comparison to that gained in [2]. A modified Pdot algorithm which was referred from [19] also is designed and applied to TRMS practical experimental setup. Its RMS error also is compared with that in [2]. Further it was observed that wherever the slope of the pitch and yaw angle is fast, the estimation error section was denser and the time taken for estimation is less and vice versa.

Acknowledgement

We are grateful to Prof. Dan Simon for providing [23] as a common resource.

References

[1] TRMS 33-949S User manual, East Sussex, U.K.: Feedback Instruments Ltd., 2006.

[2] F. A. Shaik, Shubhi Purwar, Bhanu Pratap, “Real-time implementation of Chebyshev neural network observer for twin rotor control system”, Expert Systems with Applications 38 (2011), pp. 13043-13049.

[3] R. N Crane “An application of nonlinear smoothing to submarine exercise track reconstruction”, IEEE Transactions on Automatic Control, December 1973, pp. 653-658

[4] G. Chowdhary , R. Jategaonkar, “Aerodynamic parameter estimation from flight data applying extended and unscented Kalman filter”, Aerospace Science and Technology 14,2010, pp.106-117

[5] V. Yu, A. Headley, D. Chen, “A constrained extended Kalman filter for state-of-charge estimation of a Vanadium Redox flow battery with crossover effects”, Journal of Dynamic Systems, Measurement, and Control, July 2014, vol. 136 / 041013-1.

[6] M. Barut, S. Bogosyan, and M. Gokasan, “Experimental evaluation of braided EKF for sensorless control of induction motors”, IEEE Transactions on Industrial Electronics, vol. 55, no. 2, February 2008, pp. 620-632.

[7]H. Zhu, T. Sugie, “Velocity estimation of motion systems based on low-resolution encoders”, Journal of Dynamic Systems, Measurement, and Control January 2013, vol. 135 / 011006-1.
[8] J. Zhang, G. Welch, G. Bishop, and Z. Huang,, “A two-stage Kalman filter approach for robust and real-time power system state estimation”, IEEE Transactions on Sustainable Energy, vol. 5, no. 2, April 2014, pp.629-636.
[9] M. Barczyk, A. F. Lynch, “Invariant observer design for a helicopter UAV aided inertial navigation system” IEEE Transactions on Control Systems Technology, vol. 21, no. 3, May 2013, pp. 791-806.
[10] M. Bosse and R. Zlot, “Map matching and data association for large-scale two-dimensional laser scan-based SLAM”, International Journal of Robotics Research, vol. 27 Issue 6, June 2008, pp. 667-691.
[11] E. Gartley, D. M. Bevly, “Online estimation of implement dynamics for adaptive steering control of farm tractors”, IEEE/ASME Transactions on Mechatronics, vol. 13, no. 4, August 2008, pp. 429-440.
[12]M. J. Yu, J. G. Lee, C. G. Park, “Nonlinear robust observer design for strapdown INS in-flight alignment”, IEEE Transactions on Aerospace and Electronic Systems, vol. 40, no. 3 JULY 2004, pp. 797-807.
[13] M. S. Grewal, A. P. Andrews, *Kalman Filtering Theory and Practice Using Matlab* , Wiley & Sons Inc 2001.
[14] C. Unsal, P. Kachroo, “Sliding mode measurement feedback control for antilock braking systems”, IEEE Transactions ON Control Systems Technology, vol. 7, no. 2, March 1999, pp. 271-281.
[15] Y. Song, J. W. Grizzle, “The extended Kalman filter as a local asymptotic observer for discrete-time nonlinear systems”, Journal of Mathematical Systems, Estimation and Control, vol. 5, no. 1, 1995 pp. 59-78.
[16] V. Smidl, Z. Peroutka, “Advantages of square-root extended Kalmanfilter for sensorless control of AC drives”, IEEE Transactions on Industrial Electronics, vol. 59, no. 11, November 2012, pp. 4189-4096.
[17] V.M. Becerra, P.D. Roberts and G.W. Griffiths, “Applying the extended Kalman filter to systems described by nonlinear differential-algebraic equations”, Control Engineering Practice, 9, pp. 267-281, 2001.
[18] P. S. Mayback, R. L. Jensen, D. A. Harnly, “An adaptive extended Kalman filter for target image tracking”, IEEE Transactions on Aerospace and Electronic Systems vol. AES-17, no. 2 March 1998, pp. 173-180.
[19] K.Reif F. Sonnemann, R. Unbehauen, “An EKF based nonlinear observer with a prescribed degree of stability”, Automatica, vol. 34, no.9, 1998, pp. 1119-1123.
[20] M.J. Yu, “Nonlinear robust observer design for strapdownINS in-flight alignment”, IEEE Transactions on aerospace and electronic systems, vol. 40, no. 3 July 2004, pp. 797-807.
[21] G. Mohinder, A. Angus, “Applicatuions of Kalman filtering in aerospace 1960 to present”, [Historical perspectives], Control Systems, IEEE, 30(3), pp. 69-78.
[22] D. Dochain, “State and parameter estimation in chemical and bio-chemical processes, a tutorial”, Journal of Process Control, 13 (2003), pp. 801-818.
[23] D. Simon, “Using nonlinear Kalman filtering to estimate signals”, *Embedded Systems Design*, vol. 19, no. 7, pp. 38-53, July 2006.